

# Cu(II), Ni(II), Co(II) and Cr(III) Complexes with N<sub>2</sub>O<sub>2</sub>-Chelating Schiff's Base Ligand Incorporating Azo and Sulfonamide Moieties: Spectroscopic, Electrochemical Behavior and Thermal Decomposition Studies

Hoda A. Bayoumi<sup>1,2</sup>, Abdel-Nasser M.A. Alaghaz<sup>3,4,\*</sup> and Mutlak Sh. Aljahdali<sup>5</sup>

<sup>1</sup>Chemistry Department, Girls College for Arts, Science and education, Ain Shams University, Cairo, P.O. BOX 11757, Egypt

<sup>2</sup>Chemistry Department, Faculty of Science (Girls), King Khalid University, 9004 Abha, Saudi Arabia

<sup>3</sup>Chemistry Department, Faculty of Science, Al-Azhar University, Nasr City, Cairo, Egypt

<sup>4</sup>Chemistry Department, Faculty of Science, Jazan University, Jazan, Saudi Arabia

<sup>5</sup>Chemistry Department, Faculty of Science, King Abdulaziz University, Jeddah 21589, Saudi Arabia

\*E-mail: [aalaghaz@yahoo.com](mailto:aalaghaz@yahoo.com)

Received: 12 April 2013 / Accepted: 27 May 2013 / Published: 1 July 2013

---

The Schiff base of N<sub>2</sub>O<sub>2</sub> dibasic ligand, H<sub>2</sub>L (N,N'-bis(5-(4-sulfanilamidophenylazo)salicylidene)-ethylenediamine) is prepared by the condensation of ethylenediamine with [5-(4-sulfanilamidophenylazosalicylaldehyde] in ethanol. New complexes of with metal ions Cu(II), Ni(II), Co(II) and Cr(III) are synthesized. Elemental, spectroscopic and thermal analyses as well as conductivity and magnetic susceptibility measurements are used to elucidate the structure of the newly prepared metal complexes. The structure of copper(II) complex is also assigned based upon ESR spectrum study. In metal chelates of the type 1:1 (M:L), the Schiff base behave as a di-negative N<sub>2</sub>O<sub>2</sub> tetradentate ligand. All complexes have mononuclear structure and the tetrahedral, square planar or an octahedral geometry have been proposed. The kinetic parameters for the decomposition steps have been calculated using Broido's method. Redox behaviors of the ligand and its complexes have been investigated by cyclic voltammetry at the glassy carbon electrode in 0.1 M TBATFB in DMSO.

---

**Keywords:** Azo-Schiff's base complexes, Spectroscopic study, XRD, SEM, electrochemical behavior, EDX

## 1. INTRODUCTION

The Schiff base ligands and their corresponding metal complexes have expanded enormously and include a vast area of organometallic compounds and various aspects of bioinorganic chemistry [1–3]. Schiff base ligands have been reported to show a variety of biological actions by virtue of the

azomethine linkage, which is responsible for various antibacterial, antifungal, herbicidal, clinical and analytical activities [4–6]. Transition metal complexes with oxygen and nitrogen donor Schiff bases are of particular interest [7–9], because of their ability to possess unusual configuration [10]. On the other hand, azo compounds are very important molecules and have attracted much attention in both academic and applied research [11]. Azo compounds and their metal complexes are known to be involved in a number of biological reactions, such as inhibition of DNA, RNA, and protein synthesis, nitrogen fixation, and carcinogenesis [12–13]. Also, the azo compounds and their metal–azo complexes are extremely used in dyes and data storage [14,15].

Quite recently, the Schiff base ligand derived from the condensation of 5-(4-sulfanilamidophenylazo salicylaldehyde with aniline was previously prepared and characterized [16]. As a continuation to our work, a new Schiff base, (H<sub>2</sub>L) (N,N'-bis(5-(4-sulfanilamidophenylazosalicilydene)–ethylenediamine) derived from ethylenediamine and [5-(4-sulfanilamidophenylazosalicilylaldehyde] was prepared. The obtained Schiff base ligand is reacted in 1:1 mole ratio with the appropriate metal salt (Cu(II), Ni(II), Co(II) and Cr(III)) using ethanol solvent. Interestingly, the complexes formed in which the tetradentate Schiff base ligand and lose its protons and coordinated as a dinegative N<sub>2</sub>O<sub>2</sub> species.

## 2. EXPERIMENTAL

### 2.1. Materials

All the chemicals used were of AnalaR grade and procured from Sigma–Aldrich and Fluka. Metal salts (E. Merck) were commercially available as pure samples and solvents were used as received.

### 2.2. Instrumentation

The C, H, N and S data were obtained by using a Carlo–Erba 1106 elemental analyzer. Metal contents were determined complexometrically by standard EDTA titration. The infrared spectra were recorded on a Shimadzu FT–IR spectrometer using KBr discs. The molar conductance measurements were carried out using a Sybron–Barnstead conductometer. <sup>1</sup>H NMR (300 MHz) and <sup>13</sup>C NMR (75 MHz) spectra were recorded using a Mercury–300BB. Dimethylsulfoxide, DMSO–d<sub>6</sub>, was used as a solvent and tetramethylsilane (TMS) as an internal reference. The solid reflectance spectra were measured using a Shimadzu PC3101 UV–VIS–NIR scanning spectrophotometer. Magnetic susceptibility of the metal complexes were measured by the Gouy method at room temperature using a Johnson Matthey, Alpha products, model MKI magnetic susceptibility balance and the effective magnetic moments were calculated using the relation  $\mu_{\text{eff}} = 2.828 (\chi_m \cdot T)^{1/2} B \cdot M$ , where  $\chi_m$  is the molar susceptibility corrected using Pascal's constants for diamagnetism of all atoms in the compounds. The TGA were recorded on a Shimadzu TGA–50 H. TGA was carried out in a dynamic nitrogen atmosphere (20 mL min<sup>-1</sup>) with a heating rate of 10 °C min<sup>-1</sup>. The ultraviolet spectra were recorded on a

Perkin–Elmer Lambda–3B UV–VIS spectrophotometer. The mass spectra were performed using a Shimadzu–Ge–Ms–Qp 100 EX mass spectrometer using the direct inlet system. EPR spectra of Cr(III) and Cu(II) the complexes were recorded as polycrystalline samples, at room temperature, on an E4–EPR spectrometer using the DPPH as the *g*–marker. The X-ray diffraction patterns for the obtained CT complexes were collected on a PAN analytical X'Pert PRO X-ray powder diffractometer at the Central Lab at college for girls, Ain Shams University, Egypt University, Egypt. The instrument was equipped with a Ge(III) monochromator, and a Cu K $\alpha$ 1 X-ray source with a wavelength of 0.154056 nm was used. Scanning electron microscopy (SEM) images and energy-dispersive X-ray spectroscopy (EDX) patterns were collected on a Jeol JSM-6390 instrument at a L A Jeol JSM-6510 instrument at Egyptian nuclear and radiological regulatory authority (ENRRA), Egypt. The instrument was operated at an accelerating voltage of 20 kV. Glassy carbon electrodes were prepared by first polishing them with fine wet emery papers grain size 4000 (Buehler, Lake Bluff, IL, USA) followed by a 0.1  $\mu$ m and 0.05  $\mu$ m alumina slurry on a polishing pad (Buehler, Lake Bluff, IL, USA), to give them a mirror-like appearance. The electrodes were sonicated for 5 min in water and in 50:50 (v/v) isopropyl alcohol and acetonitrile (IPA + MeCN) solution purified over activated carbon. Before the electrochemical experiments, the electrodes were dried with an argon gas stream and the solutions were purged with pure argon gas (99.999%) at least for 10 min and an argon atmosphere was maintained over the solution during experiments. Electrochemical studies of the compounds were performed in a solution of 1 mM LH2 and its complexes, in 0.1 M TBATFB in DMSO versus an Ag/Ag<sup>+</sup> (0.01 M) reference electrode using CV with a scan rate of 200 mV s<sup>-1</sup> between 1 V and –2.5 V.

### 2.3. Synthesis of the ligand (H<sub>2</sub>L)

A solution of 0.1 mol ethylenediamine (dissolved in 50 mL of ethanol) was slowly added to a solution of 0.2 mol of [5–(4–sulfanilamidophenyl)azosalicylaldehyde] in 50 mL ethanol. After the reaction mixture was refluxed for 2 h, the precipitate was cooled and collected by filtration. The precipitate was purified by washing with distilled water several times, and was then washed with ethanol, followed by recrystallization in ethanol and drying at 50 °C overnight, ligand as a yellow solid was obtained in 85% yield.

### 2.4. Preparation of the chelates

The solid chelates were prepared by the addition of hot solution  $\cong$  60 °C of the appropriate metal acetate (, Co(CH<sub>3</sub>COO)<sub>2</sub>.4H<sub>2</sub>O, Ni(CH<sub>3</sub>-COO)<sub>2</sub>.4H<sub>2</sub>O, Cu(CH<sub>3</sub>COO)<sub>2</sub>.H<sub>2</sub>O and or metal chloride (CrCl<sub>3</sub>.6H<sub>2</sub>O (1 mmol) in ethanol, 25 ml) to the well stirred hot solution ( $\cong$ 60 °C) of the Schiff base H<sub>2</sub>L (0.634 g, 1 mmol) in the same solvent (25 ml). The mixture was left under reflux with continuous stirring on a water bath for 1 h where upon the solid complexes precipitated. The resulting solid was washed with ethanol followed by diethyl ether and dried in a vacuum over anhydrous CaCl<sub>2</sub>. The analytical data of the ligand H<sub>2</sub>L and its complexes are collected in Table 1.

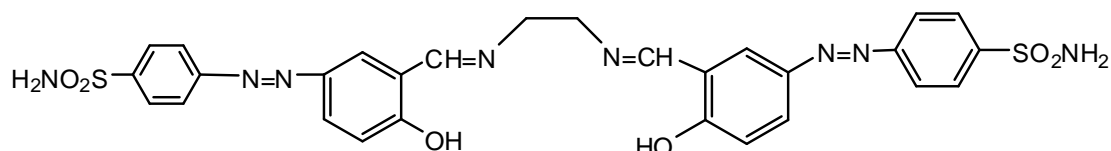
**Table 1.** Elemental analysis and some Physical measurements to ligand H<sub>2</sub>L and its complexes (1-8).

Ligand or complex	Colour	m.p. °C	Elemental Analyses (Found) calculated %					10 <sup>-3</sup> M DMFA Ohm <sup>-1</sup> cm <sup>2</sup> mol <sup>-1</sup>	
			M	C	H	N	S		Cl
H <sub>2</sub> L:(C <sub>28</sub> H <sub>26</sub> N <sub>8</sub> O <sub>6</sub> S <sub>2</sub> )	Yellow	217	–	(52.69) 52.99	(4.27) 4.13	(16.47) 17.65	(10.08) 10.10	–	–
(1)[CuL].2H <sub>2</sub> O C <sub>28</sub> H <sub>28</sub> N <sub>8</sub> O <sub>8</sub> S <sub>2</sub> Cu	Red brown	>300	(9.11) 8.68	(45.53) 45.93	(3.93) 3.85	(14.69) 15.30	(8.72) 8.76	–	28
(2)[NiL(H <sub>2</sub> O) <sub>2</sub> ].2H <sub>2</sub> O C <sub>28</sub> H <sub>32</sub> N <sub>8</sub> O <sub>10</sub> S <sub>2</sub> Ni	Dark red	>300	(8.02) 7.69	(43.75) 44.05	(3.73) 4.22	(13.22) 14.68	(8.38) 8.40	–	39
(3)[CoL(H <sub>2</sub> O) <sub>2</sub> ].2H <sub>2</sub> O C <sub>30</sub> H <sub>33</sub> N <sub>8</sub> O <sub>11</sub> S <sub>2</sub> Co	Dark red	>300	(7.70) 7.72	(44.02) 44.04	(4.21) 4.22	(14.62) 14.67	(8.39) 8.40	–	16
(4)[CrLCl(H <sub>2</sub> O) <sub>2</sub> ].2H <sub>2</sub> O C <sub>28</sub> H <sub>30</sub> N <sub>8</sub> O <sub>9</sub> S <sub>2</sub> ClCr	Red brown	>300	(6.57) 6.72	(43.28) 43.44	(4.02) 3.91	(12.85) 14.47	(8.24) 8.28	(4.19) 4.58	26

### 3. RESULTS AND DISCUSSION

#### 3.1. The ligand

H<sub>2</sub>L ligand is formed via the condensation of the azo-dye Schiff base under study with ethylenediamine. It is characterized based on elemental analyses (Table 1). The results obtained are in good agreement with those calculated for the suggested formula (Fig. 1).

**Figure 1.** The structural diagram of the H<sub>2</sub>L ligand.

The <sup>1</sup>H NMR spectra of the Schiff base ligand H<sub>2</sub>L revealed its formation by the presence of –CH=N– proton signal at  $\delta = 9.96$  ppm. Also, the <sup>1</sup>H NMR of the ligand exhibits signals at  $\delta$  (ppm) = 2.80 (s, 4H, 2CH<sub>2</sub>), 6.80–8.20 (m, 18H, 14 Ar–H+2SO<sub>2</sub>NH<sub>2</sub>) and 11.90 (brs, 2H, 2OH, exchangeable with D<sub>2</sub>O). Assignment of the <sup>13</sup>C NMR spectral data of the H<sub>2</sub>L ligand, is based on <sup>13</sup>C shifts in similar Schiff base ligand [16]. The chemical shifts for carbons of (–N=C(H)–) groups was observed between 161.7 ppm. The signal observed at 167.4 ppm is assigned to (C–O) phenolic carbon. Also, the spectrum showed peaks at 130–119 ppm corresponding to carbons of the phenyl ring.

The electron impact mass spectrum (Figure 2) of the free ligand, confirms the proposed formula by showing a peak at 634 u corresponding to the ligand moiety [(C<sub>28</sub>H<sub>26</sub>N<sub>8</sub>O<sub>6</sub>S<sub>2</sub> atomic mass 634.69 u]. The series of peaks in the range, i.e. 56, 69, 77, 96, 109, 120, 135, 149, 167, 172, 190, 221, 248 and 494 u, attributable to different fragments of the ligand. These data suggest the condensation of keto group with amino group. The molecular ion peak (634 u) is in good agreement with the suggested

molecular formula indicated from elemental analyses. The mass spectrum of the ligand (H<sub>2</sub>L) shows the fragmentation pattern in Figure 3.

Further insight concerning the structure of the ligand is obtained from IR, UV-vis. The IR and UV-vis measurements, of H<sub>2</sub>L ligand will be discussed with its metal complexes.

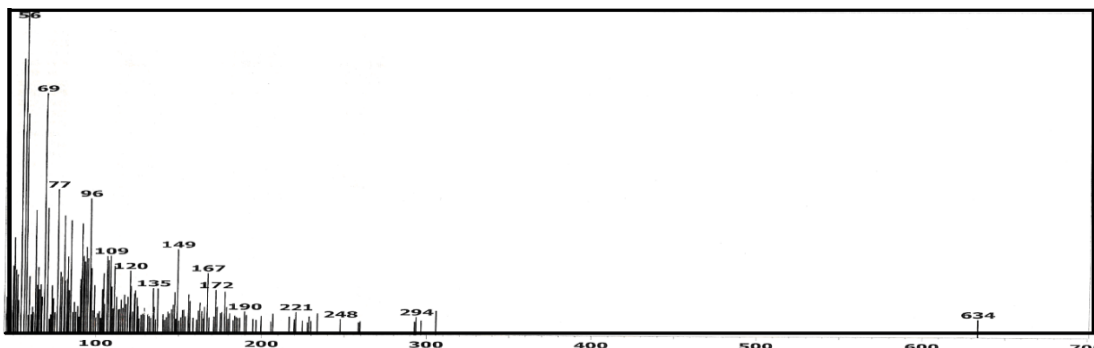


Figure 2. Mass spectrum of the H<sub>2</sub>L ligand.

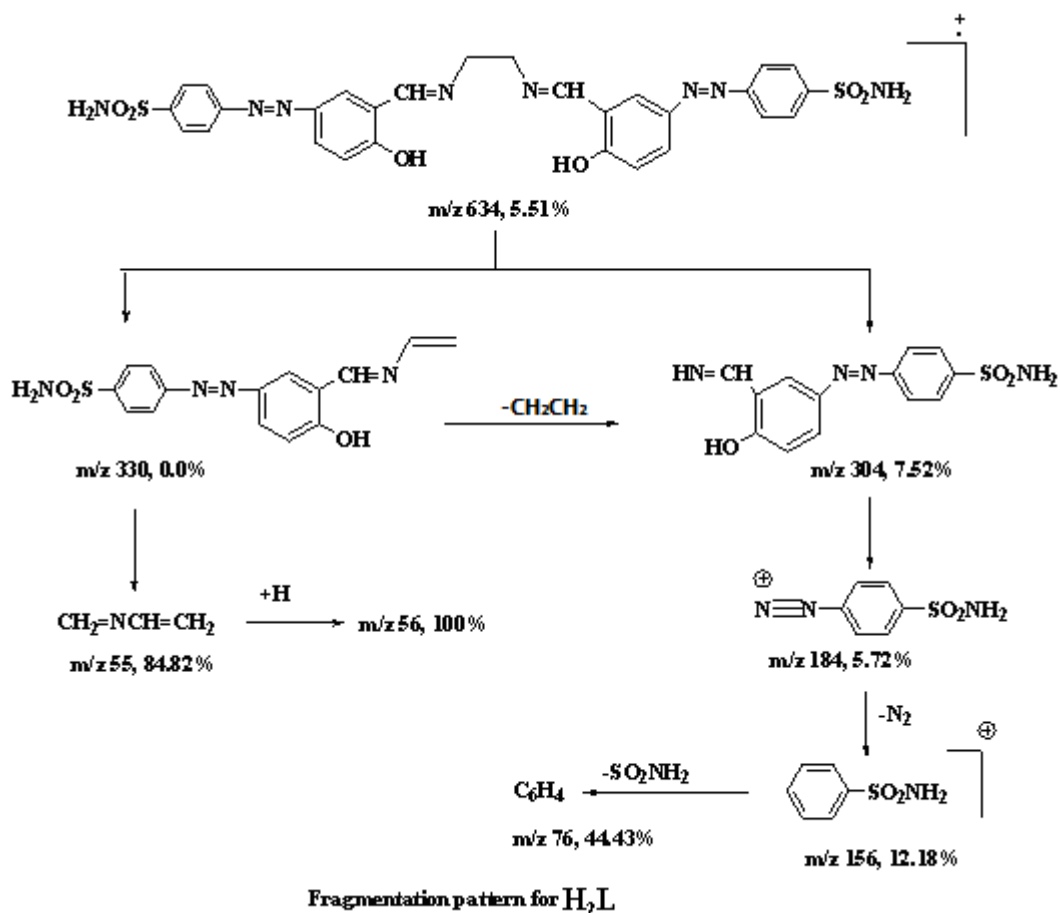


Figure 3. Fragmentation pathways of the H<sub>2</sub>L ligand.

### 3.2. Metal complexes

Following the successful preparation of the ligand, attention was directed towards the chemical behaviour of the ligand H<sub>2</sub>L towards transition metal ions. The metal ions selected for this purpose were Cr(III), Co(II), Ni(II) and Cu(II).

When a mixture of 1 mole of H<sub>2</sub>L ligand in dry ethanol was reacted with 1 mole of the metal salts in dry ethanol, a change in colour was observed and the complex compounds precipitated. The products were purified by washing with ethanol, and gave elemental analyses compatible with the suggested formulae given in Table 1. On the basis of elemental analysis data (Table 1), all the complexes have the general composition [CrLCl(H<sub>2</sub>O)].2H<sub>2</sub>O, and [M(L)(H<sub>2</sub>O)<sub>n</sub>].2H<sub>2</sub>O in which M = Co(II), n= 2; Ni(II), n= 2; Cu(II), n= zero ions and L is N,N'-bis(5-(4-sulfanilamidophenylazo-salicylidene)-ethylenediamine). The obtained complexes are powder solids which are stable in air and decompose above 300 °C (Table 1). Further, confirmation of the proposed structures of the chelates of the Schiff base of azo-dye with metal salts was done using different physico-chemical methods shown below.

#### 3.2.1. Molar conductivities of metal complexes

Molar conductance ( $\Lambda M$ ) measurements of the complexes (Table 1), carried out using DMSO as the solvent at the concentration of 10<sup>-3</sup> M, indicate non-electrolyte behaviour of the complexes and conductivity values were found in the range 11–39 Ω<sup>-1</sup> cm<sup>2</sup> mol<sup>-1</sup> [17] (Table 1). Thus the complexes may be formulated as [CrLCl(H<sub>2</sub>O)].2H<sub>2</sub>O and [M(L)(H<sub>2</sub>O)<sub>n</sub>].2H<sub>2</sub>O in which M = Co(II), n= 2; Ni(II), n= 2; Cu(II), n= zero ions.

#### 3.2.2. IR spectra and mode of bonding

The infrared spectra assignment of the proposed structures of the Schiff base of azo-dye complexes was made through consideration of their infrared spectra. The coordinated stretching vibration bands of the isolated products were assigned by using a comparison method of infrared spectra comparing the spectra of the free ligand and its metal complexes. The IR spectra of the free ligand and metal complexes (Table 2) were carried out in the range 4000–400 cm<sup>-1</sup>. The IR spectra of the complexes show a sharp band in the range 1605–1613 cm<sup>-1</sup>, attributed to ν(-C=N-), which is shifted to higher frequency on going from the free ligand (at 1643 cm<sup>-1</sup>) to the complexes. This is indicative of the coordination of the imine nitrogen to the metal. In the far IR spectra of all the complexes, the non-ligand bands observed at 455–410 cm<sup>-1</sup> region assigned to ν(M-N) stretch [18]. The disappearance of the free ligand ν(OH) band around 3424 cm<sup>-1</sup> in the spectra of all complexes indicating deprotonation of organic ligand prior to coordination. On the other hand, the ν(C-O), which occur at 1294 cm<sup>-1</sup> for the ligand, was moved to higher frequencies, 1410–1302 cm<sup>-1</sup> after complexation, this shift confirms the participation of phenolic oxygen of the ligand in C-O-M bond formation [19]. Conclusive evidence regarding the bonding of oxygen to the metal ions is provided by the occurrence of bands at 530–504 cm<sup>-1</sup> region due to ν(M-O) [20]. The ν(NH) mode of the

sulfonamide group/amino group in the uncoordinated Schiff base remains unchanged in the spectra of their complexes. This suggests that the sulfonamide nitrogen or amino group is not taking part in coordination. The bands, in this ligand, due to  $\nu_{as}(-SO_2)$  and  $\nu_s(-SO_2)$  appear at 852 and 645  $cm^{-1}$ , respectively. These remain almost unchanged in the spectra of complexes, indicating that sulfonamide oxygens are not participating in coordination [21]. In the free ligand, the sharp band observed at 1512  $cm^{-1}$  is due to  $\nu(-N=N-)$  stretching frequency of azo-dye. In all complexes, this band remains quite unchanged confirming the noninvolvement of the azo-dye nitrogen in complex formation [22]. The bands in the range 788–836  $cm^{-1}$  and 624–633  $cm^{-1}$  appeared in the spectra of these complexes which may be assigned to  $\rho r(H_2O)$  and  $\rho w(H_2O)$  [23]. Finally, the assignment of the nature of water molecules associated with the complex formation under study was much more complicated as ligands vibrations interfere in this region. The thermal data confirms the nature of water molecule to be lattice/coordinated. The thermal study will be discussed in detailed manner later.

**Table 2.** Infrared wave numbers ( $cm^{-1}$ ) and tentative band assignments for the synthesized ligand, ( $H_2L$ ) and its metal complexes (1-8).

No.	$\nu_{OH}$ phenolic/ $H_2O$	$\nu_{H_2O}$ $\rho r$ &( $\rho w$ )	$\nu_{NH_2}$ asy&(sy)	$\nu_{NH}$ asy&(sy)	$\rho_{NH}$	$\nu_{C=N}$	$\nu_{-N=N}$	$\nu_{SO_2}$ asy&(sy)	$\nu_{C-O}$ (phenolic)	$\nu_{M-N}$	$\nu_{M-O}$
$H_2L$	3424br	–	3376m (3250s)	3270m (3193s)	1562m	1643s	1512w	580m (643s)	1294m	–	–
(1)	3317br	780m (624m)	3377m (3254s)	3274m (3199s)	1560m	1612s	1510w	580m (644m)	1309m	451m	504w
(2)	3329br	782m (625m)	3378m (3268s)	3276m (3194s)	1568m	1608s	1508w	582m (645m)	1328m	451m	519w
(3)	3300br	836m (632m)	3386m (3254s)	3277m (3190s)	1568m	1610s	1508w	581m (642m)	1329w	455w	512w
(4)	3300br	783m (628s)	3376m (3263s)	3277m (3198s)	1560w	1605s	1510w	583m (648s)	1326m	444m	504w

### 3.2.4. Magnetic susceptibility and electronic spectra measurements

The electronic spectra of ligand and their complexes (Table 3) were displayed in DMF. The spectra of complexes are dominated by intense intra-ligand charge transfer bands. The spectrum of  $H_2L$  shows an intense absorption band at 36,496–35,971  $cm^{-1}$  region assigned to  $n \rightarrow \pi^*$  transition of azomethine groups [16, 23].

Chromium(III) complex shows magnetic moments corresponding to three unpaired electrons, i.e. 3.83 B.M., expected for high-spin octahedral chromium(III) complexes [16,23-25]. Six coordinated Cr(III) complexes with octahedral symmetry show three spin allowed bands in the range of 18,000–30,000  $cm^{-1}$ . While the complex under study shows four bands in the range of 16,953–38,463  $cm^{-1}$ . This type of complex may have either  $C_{4v}$  or  $D_{4h}$  symmetry. The Cr(III) complex display bands at 16,945, 24,563, 27,476, and 38,468  $cm^{-1}$ , respectively (Fig. 4, Table 5). These bands may be assigned to  ${}^4B_{1g} \rightarrow {}^4E^a_g(v_1)$ ,  ${}^4B_{1g} \rightarrow {}^4B_{2g}(v_2)$ ,  ${}^4B_{1g} \rightarrow {}^4E^b_g(v_3)$  and  ${}^4B_{1g} \rightarrow {}^4A_{1g}(v_4)$  transitions, respectively,

arising from the lifting of the degeneracy of the orbital triplet (in octahedral symmetry) in the order of increasing energy and assuming  $D_{4h}$  symmetry [23].

Co(II) complex shows magnetic moment at 3.94 B.M. corresponding to three unpaired electrons. The electronic spectrum of the Co(II) complex displays three bands at 10,690, 15,185 and 25,049  $\text{cm}^{-1}$  (Fig. 5). These bands may be assigned to following transitions  ${}^4T_{1g} \rightarrow {}^4T_{2g}(F)(\nu_1)$ ,  ${}^4T_{1g} \rightarrow {}^4A_{2g}(F)(\nu_2)$  and  ${}^4T_{1g} \rightarrow {}^4T_{1g}(P)(\nu_3)$ , respectively. The position of bands suggest octahedral geometry of Co(II) complex [16, 23].

The nickel(II) complex shows magnetic moment 2.92 B.M. corresponding to two unpaired electrons [16, 23]. Electronic spectrum displays bands at 11,357, 15,802 and 21,489  $\text{cm}^{-1}$  (Fig. 5) These bands may be assigned to  ${}^3A_2(F) \rightarrow {}^3T_2(F)(\nu_1)$ ,  ${}^3A_2(F) \rightarrow {}^3T_1(F)(\nu_2)$  and  ${}^3A_2(F) \rightarrow {}^3T_1(P)(\nu_3)$  transitions, respectively. It suggests tetrahedral geometry of Ni(II) complex [16, 23].

The observed magnetic moment of the Cu(II) complex is 1.96 B.M., which confirms the square planar structure of this complex. Electronic spectrum of the copper(II) complex displays bands at 10,167, 18,534, and 30,373  $\text{cm}^{-1}$ . First two bands may be assigned to the transitions:  ${}^2B_{1g} \rightarrow {}^2A_{1g}(dx^2-y^2 \rightarrow dz^2)(\nu_1)$ ,  ${}^2B_{1g} \rightarrow {}^2B_{2g}(dx^2-y^2 \rightarrow d_{zy})(\nu_2)$ , respectively and third band may be due to charge transfer.

**Table 3.** Molar conductance, magnetic moment and electronic spectral data of the complexes

Complex	Geometry	$\mu_{\text{eff}}$ (B.M.)	Band assignments	$\lambda_{\text{max}}(\text{cm}^{-1})$
[Co(L)(H <sub>2</sub> O) <sub>2</sub> ].2H <sub>2</sub> O	Octahedral	3.94	${}^4T_{1g} \rightarrow {}^4T_{2g}(F)$ ${}^4T_{1g} \rightarrow {}^4A_{2g}(F)$ ${}^4T_{1g} \rightarrow {}^4T_{1g}(P)$	10,690 15,185 25,049
[Ni(L)(H <sub>2</sub> O) <sub>2</sub> ].2H <sub>2</sub> O	Tetrahedral	2.92	${}^3A_2(F) \rightarrow {}^3T_2(F)$ ${}^3A_2(F) \rightarrow {}^3T_1(F)$ ${}^3A_2(F) \rightarrow {}^3T_1(P)$	11,357 15,802 21,489
[Cu(L)].2H <sub>2</sub> O	Octahedral	1.96	${}^2B_{1g} \rightarrow {}^2A_{1g}(dx^2-y^2 \rightarrow dz^2)(\nu_1)$ ${}^2B_{1g} \rightarrow {}^2B_{2g}(dx^2-y^2 \rightarrow d_{zy})(\nu_2)$	10,167 18,534

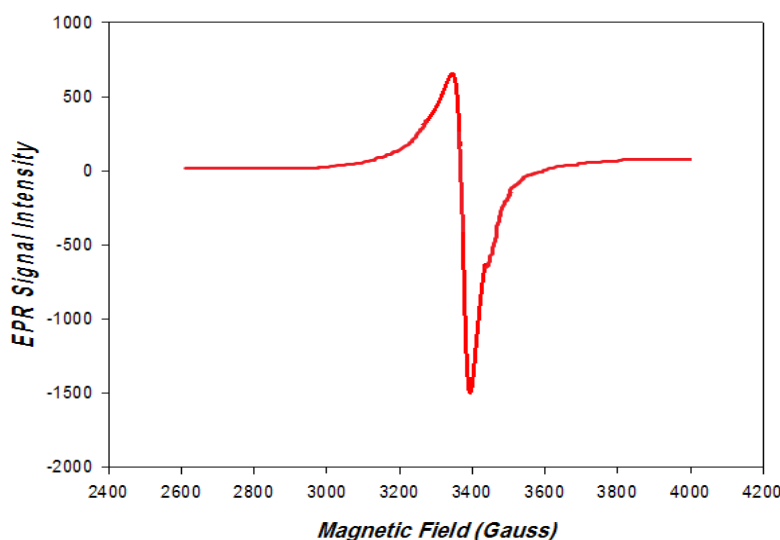


**Figure 4.** ESR spectrum of [Cu(L)].2H<sub>2</sub>O complex.

**Table 4.** ESR parameters of [Cu(L)]2H<sub>2</sub>O complex

Complex	$g_{\parallel}$	$g_{\perp}$	$g_{\text{iso}}$	$A_{\parallel} \times 10^{-4} (\text{cm}^{-1})$	$g_{\parallel}/A_{\parallel}$	G	$\alpha^2$	$\beta^2$
[Cu(L)].2H <sub>2</sub> O	2.23	2.02	2.09	164.27	135	2.24	0.66	0.53

The complex may have tetragonal geometry [25]. EPR spectrum of Cu(II) complex was recorded at room temperature as polycrystalline samples and in DMF solution, on the *x*-band at 9.1 GHz under the magnetic field strength 3400 G. Polycrystalline spectrum shows a well-resolved anisotropic broad signal (Fig. 4, Table 4). The analysis of spectra give  $g_{\parallel} = 2.23$  and  $g_{\perp} = 2.02$ . The trend  $g_{\parallel} > g_{\perp} > 2.0023$ , observed for the complex, under study, indicates that the unpaired electron is localized in  $dx^2-y^2$  orbital of the Cu(II) ion and the spectral features are characteristic for axial symmetry. Tetragonal elongated geometry is thus confirmed for the aforesaid complex[25].

### 3.2.5. Ligand field parameters

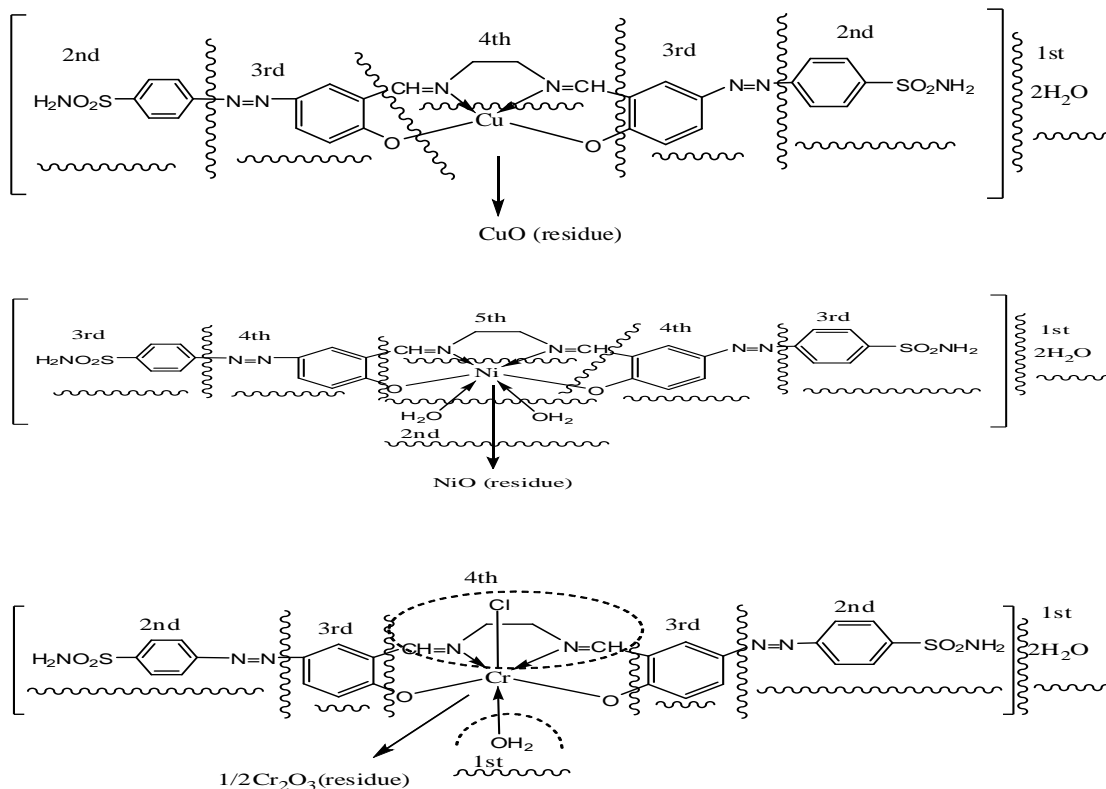
Various ligand parameters were calculated for the complexes and are listed in Table 5. The value  $Dq$  in Co(II) complexes was calculated from transition energy ratio diagram using the  $\nu_3/\nu_2$  ratio. The Nephelauxetic parameter  $\beta$  was calculated by using the relation  $\beta = B(\text{complex})/B(\text{free ion})$ , where  $B$  free ion for Cr(III), Co(II) and Ni(II) is 921, 963, and 906  $\text{cm}^{-1}$ . The  $\beta$  value lies in the range 0.37–0.94. These values indicate that the appreciable covalent character of metal ligand  $\sigma$  bond [16, 23, 25].

**Table 5.** Ligand field parameters of the complexes

Complex	$Dq (\text{cm}^{-1})$	$B(\text{cm}^{-1})$	$\beta$	LFSE ( $\text{kJmol}^{-1}$ )	$F_2$	$F_4$	$C$	$\nu_2/\nu_1$
[CrCl(H <sub>2</sub> O)].2H <sub>2</sub> O	1689	921	0.86	214.23	–	–	–	1.44
[Co(L)(H <sub>2</sub> O) <sub>2</sub> ].2H <sub>2</sub> O	1182	906	0.37	96.43	–	–	–	1.42
[Ni(L)(H <sub>2</sub> O) <sub>2</sub> ].2H <sub>2</sub> O	798	–	0.94	113.82	–	–	–	1.39

### 3.2.6. Thermal analysis

The thermal degradation of Cu(II), Ni(II) and Cr(III) complexes was studied using thermogravimetric techniques and a temperature range of 25–800 °C. The thermal stability data are listed in Table 6. The data from the thermogravimetric analysis clearly indicated that the decomposition of the complexes proceeds in four or five steps. Water molecules were lost in between 50 and 300 °C and metal oxides were formed above 600 °C for Cu(II), Ni(II) and Cr(III) complexes. For these complexes, the removal of water can proceed in one or two steps. All complexes lost hydration water between 50 and 120 °C, and then the coordinated water molecule was lost above  $\geq 180^\circ$ . The decomposition was complete at  $\geq 600^\circ\text{C}$  for all complexes. The degradation pathway for all complexes may be represented as follows:



3.2.7. Kinetic studies

**Table 6.** Decomposition steps with the temperature range and weight loss for H<sub>2</sub>L complexes.

Compound	Decomposition step	Temperature range (°C)	removes species	wt loss	
				% (Cald.)	% Found
[CuL].2H <sub>2</sub> O	1 <sup>st</sup>	53–104	– 2H <sub>2</sub> O	4.92	4.87
	2 <sup>nd</sup>	190–314	–(C <sub>12</sub> H <sub>8</sub> N <sub>2</sub> O <sub>4</sub> S <sub>2</sub> )	42.11	41.92
	3 <sup>rd</sup>	315–593	–(C <sub>12</sub> H <sub>6</sub> N <sub>4</sub> O)	30.34	30.02
	4 <sup>th</sup>	593–747	–(C <sub>4</sub> H <sub>6</sub> N <sub>2</sub> )	11.21	11.11
	Residue	747–800	–CuO (residue)	10.86	10.79
[NiL(H <sub>2</sub> O) <sub>2</sub> ].2H <sub>2</sub> O	1 <sup>st</sup>	44–113	–2H <sub>2</sub> O	4.71	4.62
	2 <sup>nd</sup>	114–197	–2H <sub>2</sub> O	4.71	4.68
	3 <sup>rd</sup>	382–448	–(C <sub>12</sub> H <sub>12</sub> N <sub>2</sub> O <sub>4</sub> S <sub>2</sub> )	40.91	40.87
	4 <sup>th</sup>	448–642	–(C <sub>12</sub> H <sub>6</sub> N <sub>4</sub> O)	29.10	28.98
	5 <sup>th</sup>	642–737	–(C <sub>4</sub> H <sub>6</sub> N <sub>2</sub> )	10.75	10.71
	Residue	737–800	–NiO	9.78	9.73
[CrLCl(H <sub>2</sub> O)].2H <sub>2</sub> O	1 <sup>st</sup>	44–113	–3H <sub>2</sub> O	6.97	6.97
	2 <sup>nd</sup>	114–197	–(C <sub>12</sub> H <sub>12</sub> N <sub>2</sub> O <sub>4</sub> S <sub>2</sub> )	47.58	47.49
	3 <sup>rd</sup>	197–382	–(C <sub>12</sub> H <sub>6</sub> )	19.37	19.32
	4 <sup>th</sup>	197–382	–(C <sub>4</sub> H <sub>6</sub> N <sub>2</sub> O <sub>0.5</sub> Cl)	16.22	16.18
	Residue	737–800	– 1/2Cr <sub>2</sub> O <sub>3</sub>	9.82	9.79

In the present investigation, the general thermal behaviors of the complexes in terms of stability ranges, peak temperatures and values of kinetic parameters, are shown in Table 7. All the well-defined stages were selected to study the decomposition kinetics of the complexes. Various methods exist for studying the thermal decomposition of complexes. In this work, Broido's method was utilized [26].

The activation energy  $E^*a$  in the different stages is in the range of 31.14–333.95 kJmol<sup>-1</sup>. The corresponding values of the entropy of activation,  $\Delta S^*$ , were in the range of -0.0121 to -0.323 kJmol<sup>-1</sup>K<sup>-1</sup>. The  $\Delta S^*$  values for complexes were found to be negative. This indicates that the activated complex is more ordered than the reactants and/or the reactions are slow. The enthalpy of activation,  $\Delta H^*$ , values were in the range of 28.24–321.21 kJmol<sup>-1</sup>. The positive values of  $\Delta H^*$  means that the decomposition processes are endothermic. The corresponding values of the free energy of activation,  $\Delta G^*$ , were in the range of 90.78–282.26 kJmol<sup>-1</sup>.

**Table 7.** Kinetic Parameters evaluated by Broido's equation for the prepared complexes.

complex	peak	Mid Temp(K)	Ea KJ/mol	A (S <sup>-1</sup> )	$\Delta H^*$ KJ/mol	$\Delta S^*$ KJ/mol.K	$\Delta G^*$ KJ/mol
[CuL].2H <sub>2</sub> O	1 <sup>st</sup>	328.04	49.21	5.46x10 <sup>5</sup>	46.89	-0.1258	98.24
	2 <sup>nd</sup>	518.29	112.58	9.78x10 <sup>9</sup>	111.58	-0.0721	146.28
	3 <sup>rd</sup>	813.17	87.58	2.12x10 <sup>3</sup>	76.39	-0.323	244.68
	4 <sup>th</sup>	946.89	172.36	5.32x10 <sup>6</sup>	162.04	-0.2140	275.25
[NiL(H <sub>2</sub> O) <sub>2</sub> ].2H <sub>2</sub> O	1 <sup>st</sup>	358.38	31.14	2.57x10 <sup>2</sup>	26.47	-0.2121	90.78
	2 <sup>nd</sup>	436.76	48.84	4.66x10 <sup>3</sup>	42.36	-0.1754	134.86
	3 <sup>rd</sup>	635.47	182.88	4.74 x10 <sup>14</sup>	175.26	-0.0121	178.78
	4 <sup>th</sup>	694.54	152.56	3.56x10 <sup>9</sup>	145.32	-0.0802	198.24
	5 <sup>th</sup>	874.24	154.69	4.98x10 <sup>6</sup>	147.44	-0.1340	257.17
	6 <sup>th</sup>	955.87	333.95	2.49x10 <sup>18</sup>	321.21	-0.0642	271.22
[CrLCl(H <sub>2</sub> O)].2H <sub>2</sub> O	1 <sup>st</sup>	377.05	33.35	7.67 x10 <sup>2</sup>	28.24	-0.2249	112.34
	2 <sup>nd</sup>	586.12	68.23	2.48 x10 <sup>5</sup>	75.26	-0.1865	187.87
	3 <sup>rd</sup>	748.11	111.86	4.58 x10 <sup>4</sup>	104.68	-0.1546	233.29

### 3.2.8. Powder X-ray diffraction

**Table 8.** Crystallographic data for the Schiff base complexes [Cu(L)].2H<sub>2</sub>O and [Co(L)(H<sub>2</sub>O)<sub>2</sub>].2H<sub>2</sub>O.

Data	[Cu(L)].2H <sub>2</sub> O	[Co(L)(H <sub>2</sub> O) <sub>2</sub> ].2H <sub>2</sub> O
Empirical formula	C <sub>32</sub> H <sub>28</sub> Cl <sub>2</sub> N <sub>4</sub> NiO <sub>6</sub> S <sub>2</sub>	C <sub>32</sub> H <sub>24</sub> Cl <sub>2</sub> CuN <sub>4</sub> O <sub>4</sub> S <sub>2</sub>
Formula weight (g/mol)	732.25	804.69
Wavelength(Å)	1.54056	1.54056
Crystal system	Tetragonal	Cubic
Space group	P4/m	P4/m
Unit cell dimensions(Å,°)		
a(Å)	7.014585	15.9862
b(Å)	7.014575	15.9862
c(°)	15.875214	15.9862
α(°)	90	90
β(°)	90	90
γ(°)	90	90
Volume (Å <sup>3</sup> )	1108.67	6045.58
(Calc.) densit (g/cm <sup>-3</sup> )	1.8562	1.2435

2θ range	13.47–56.48	16.23–64.87
Limiting indices	0 ≤ h ≤ 3, 0 ≤ k ≤ 1, 1 ≤ l ≤ 7	3 ≤ h ≤ 10, 1 ≤ k ≤ 6, 3 ≤ l ≤ 10
Z	2	6
Rf	0.0000787	0.000023
Temperature (K)	298	298

Single crystals of the complexes could not be prepared to get the XRD and hence the powder diffraction data were obtained for structural characterization. Structures determination by X-ray powder diffraction data have gone through a recent surge since it have becomes important to get to the structural information of materials, which do not yield good quality single crystals. The indexing procedures were performed using (CCP4, UK) CRYSFIRE program [27] giving cubic crystal system for [Co(L)(H<sub>2</sub>O)<sub>2</sub>].2H<sub>2</sub>O (Fig. 10a) having M(6) = 15, F(6) = 7 and tetragonal crystal system for [Cu(L)].2H<sub>2</sub>O (Fig. 10b) having M(9) = 11, F(6) = 6 as the best solutions. Their cell parameters are shown in Table 8.

### 3.2.9. SEM and EDX studies

SEM is a simple method can be used to check the deposited samples which clearly indicated that the nanoparticles have been formed. According to the image of SEM, the diameter of the residual sample for Co(II) is about 460 nm. Figure 5 shows the scanning electron microscopy picture of Co(II) complex particles at 600 °C. By comparison between the residual products in this study and the Co(II) oxides nanoparticles in the literature [28,29], it is obvious that the particles 460 nm diameter are.

The results by energy dispersive x-ray analysis (EDX) have indicated that there are cobalt and oxygen peaks, which meant there were oxygen contamination or the deposited products were copper or cobalt oxides as shown in Fig. 5.

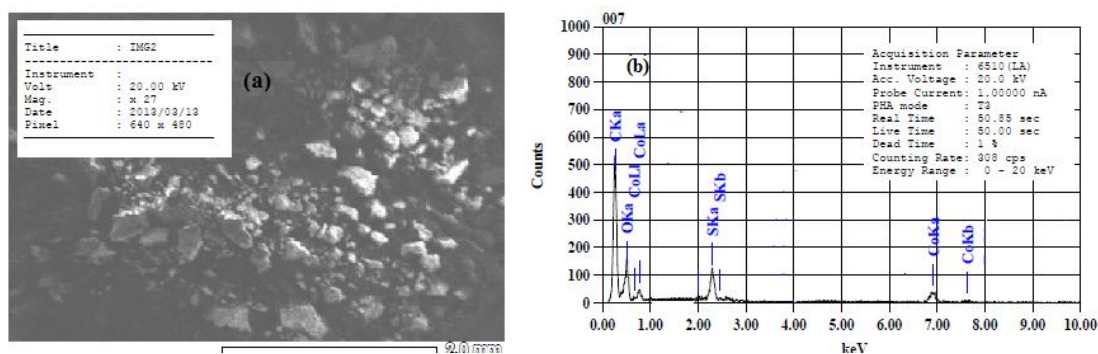


**Figure 5.** (a) SEM image of [Co(L)(H<sub>2</sub>O)<sub>2</sub>].2H<sub>2</sub>O and (b) EDX spectrum of [Co(L)(H<sub>2</sub>O)<sub>2</sub>].2H<sub>2</sub>O complex.

### 3.3. Electrochemical studies

The electrochemical properties of the ligand, H<sub>2</sub>L and its metal complexes were investigated in DMSO solution containing 0.1 M TBATFB as a supporting electrolyte by cyclic voltammetry. All

the measurements were carried out in 1 mM solutions of free ligand and its complexes at room temperature, in the potential range from +1 to -2.5 V with a scan rate of 200 mV s<sup>-1</sup>.

First, we carried out the voltammetric measurements of azo-dye in order to compare its redox behavior with those of the ligand and its metal complexes and thus assign the nature of the redox processes. The main difference of these two voltammograms is the presence of only one reduction peak in the Ac voltammogram (-2.03 V) but two reduction peaks in the voltammogram of H<sub>2</sub>L (-1.84 and -2.11 V). Comparison of the redox data of H<sub>2</sub>L with azo-dye implies that the first reduction process probably corresponds to the imino group of hydroxyl moieties (E<sub>pc</sub> = -1.83 V) while the second reduction process corresponds to the azo-dye moiety in H<sub>2</sub>L.

The reversible waves in the positive potential region are always observed for all complexes of H<sub>2</sub>L with small differences in peak potentials and peak currents depending on the stability of the complexes and the kinetics of the electron transfer. For Ni(II) complex, the reduction wave (E<sub>pc</sub> = -1.54 V) corresponding to Ni(II)/Ni(I) reaction is obtained [30,31] in the cathodic potential region, in addition to the ligand peak at -1.80 V.

For the Cu(II) complex, the reversible wave at E<sub>1/2</sub> = -0.08 V and an irreversible peak at -0.73 V correspond to the Cu(II)/Cu(I) and Cu(I)/Cu(0) couples, respectively, in addition to the ligand peaks at -1.29 V and -2.13 V [32,33]. The reversible Cu(II)/Cu(I) wave has an adsorptional character with almost symmetric cathodic and anodic peaks with a peak separation value of 10 mV. The reversible character indicates that both Cu(II) and Cu(I) complexes of H<sub>2</sub>L are stable at the electrode surface and in DMSO. As can be inferred from the irreversible character of the peak at -0.73 V, the Cu(I) complex is probably destroyed during the reduction of Cu(I) to Cu(0) in the complex.

Comparison of the voltammetric data of Ni(II) complex and Cu(II) complex with that of H<sub>2</sub>L suggests that the reduction peaks at -1.80 V and -1.29 V are due to oxime-based processes. These ligand-based reduction processes, especially the azomethine-based reduction process of Ni(II) complex, occurs at less negative potentials than those of H<sub>2</sub>L. This behavior was also observed in Ni(II) complex presumably due to negative charge transfer from ligand to metal during the formation of metal complexes [34].

For Co(II) complex the absence of the reduction peak of the imino group indicates that, owing to the lack of transferable hydroxylic protons, the reduction potentials of the dianionic ligands have been shifted beyond the lower limit of the potential interval considered in the experimental measurements [35]. The CV wave for the process Co(II)/Co(I) falls at potentials near -1.82 V.

In these complexes, the cyclic voltammetric M(II)/M(I) reduction process was observed at -1.74 V and -1.59 V and oxime group reductions were observed at -2.17 V and -2.24 V, respectively. For all complex CV measurements, at different scan rates in the range of 50–800 mV s<sup>-1</sup>, the E<sub>pc</sub> values appear to be only slightly dependent upon the scan rate. Furthermore, in all cases a linear relationship between the cathodic peak current (i<sub>pc</sub>) and the square root of the scan rate was observed. This fact implies that these electrochemical processes are mainly diffusion-controlled.

### 3.4. Structural interpretation

The structures of the prepared complexes are given in Fig. 6.

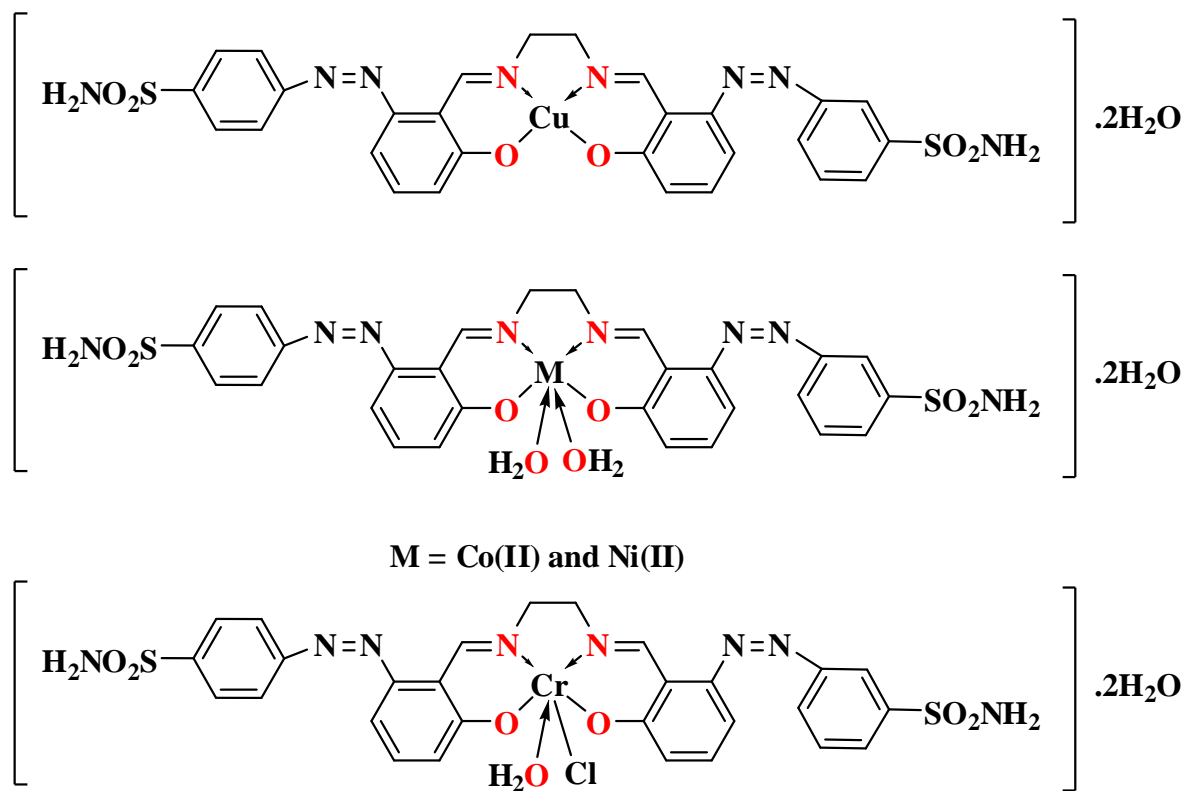


**Figure 6.** Proposed structure of complexes.

## References

1. T.T. Tidwell, *Angew Chem. Int. Ed.* 47 (2008) 1016–1020.
2. N.E. Borisova, M.D. Reshetova, Y.A. Ustynyuk, *Chem. Rev.* 107(1) (2007) 46–79.
3. A.A. Jarrahpour, M. Motamedifar, K. Pakshir, N. Hadi, M. Zarei, *Coord. Chem. Rev.* 253 (2009) 235–249.
4. S.K. Hadjidakou, N. Hadjiliadis, *Coord. Chem. Rev.* 253 (2009) 235–249.
5. A. Garoufis, S.K. Hadjidakou, N. Hadjiliadis, *Coord. Chem. Rev.* 253 (2009) 1384–1397.
6. H. Naeimi, K. Rabiei, F. Salimi, *Dyes & Pigments* 75 (2007) 294–297.
7. N.E. Borisova, M.D. Reshetova, Y.A. Ustynyuk, *Chem. Rev.* 107 (2007) 46–79.
8. A. Shokrollahi, M. Ghaedi, M. Montazerzohori, A.H. Kianfar, H. Ghaedi, N. Khanjari, S. Noshadi, S. Joybar, *E-Journal of Chemistry* 8(2) (2011) 495–506.
9. O. Kocyigit, E. Gulcur, *J. Incl. Phenom. Macrocycl. Chem.* 67 (2010) 287–293.
10. A. Golcu, M. Tumer, H. Demirelli, R.A. Wheatley, *Inorg. Chim. Acta* 358 (2005) 1785–1797.
11. H. Nishihara, *Bull. Chem. Soc. of Japan* 77 (2004) 407–428.
12. M. Badea, A. Emandi, D. Marinescu, E. Cristurean, R. Olar, A. Braileanu, P. Budrugaec, E. Segal, *J. Therm. Anal. Calorim.* 72 (2003) 525–531.
13. E. Ispir, *Dyes & Pigments* 82 (2009) 13–19.
14. R. Asgari-sabet, H. Khoshsima, *Dyes & Pigments* 87 (2010) 95–99.
15. Y.D. Kim, J.H. Cho, C.R. Park, J.H. Choi, C. Yoon, J.P. Kim, *Dyes & Pigments* 89 (2011) 1–8.
16. A.M.A. Alaghaz, H.A. Bayoumi, Y.A. Ammar, S.A. Aldhlmani, *J Molec Struct* 1035 (2013) 383–399.
17. S. Chandra, N. Gupta, R. Gupta, S.S. Bawa, *Spectrochim. Acta A* 62 (2005) 552–556.
18. G.G. Mohamed, Z.H. Abd El-Wahab, *Spectrochim. Acta A* 61 (2005) 1059–1068; G.G. Mohamed, *Spectrochim. Acta A* 64 (2006) 188–195; G.G.; Mohamed, M. M.; Omar, A. A. Ibrahim, *Eur. J. Med. Chem.* 44 (2009) 4801–4812.

19. K. Nakamoto, *Infrared and Raman Spectra of Inorganic and Coordination Compounds*, fourth ed., Wiley, New York, 1980.
20. A.A. El-Sherif, T.M.A. Eldebss, *Spectrochim. Acta A* 79 (2011) 1803–1814.
21. A.M. Tawfik, M.A. El-ghamry, S.M. Abu-El-Wafa, N.M. Ahmed, *Spectrochim. Acta A* 97 (2012) 1172–1180.
22. K. Nejati, Z. Rezvani, M.Seyedahmadian, *Dyes & Pigments* 83 (2009) 304–311.
23. A.M.A. Alaghaz, R.A. Ammar, *Eur. J. Med. Chem.* 45 (2010) 1314–1322.
24. C.M. Sharaby, *Spectrochim. Acta A* 66 (2007) 1271–1278.
25. S. Chandra, S.Verma, *J. Inorg. Nucl. Chem.* 37 (1975) 2429–2434.
26. A. Broido, F. Shafizadeh, K. Sarkanen, D. Tilman, *Thermal Uses and Properties of Carbohydrates and Lignites*, Academic Press, New York (1976)
27. R. Shirley *The CRYSFIRE System for Automatic Powder Indexing: User's Manual*, Lattice Press, 2002.
28. M. Salavati-Niasari, F. Mohandes, F. Davar, M. Mazaheri, M. Monemzadeh, N. Yavarinia, *Inorg. Chim. Acta* 362 (2009) 3691–3697.
29. B.P. Baranwal, T. Fatma, A. Varma, A.K. Singh, *Spectrochim. Acta A* 75 (2010) 1177–1180.
30. V.A. Sawant, B.A. Yamgar, S.K. Sawant, S.S. Chavan, *Spectrochim. Acta A* 74(2009) 1100-1106.
31. A. Kılıç, E. Tas, I. Yılmaz, *J. Chem. Sci.* 121 (2009) 43-52.
32. S. Zolezzi, E. Spodine, A. Decinti, *Polyhedron* 21 (2002) 55-59.
33. M. Kandaz, A. Koca, A.R. Özkaya, *Polyhedron* 23 (2004) 1987-1992.
34. M. Özer, M. Kandaz, A.R. Özkaya, M. Bulut, O. Güney, *Dyes Pigments* 76 (2008) 125-131.
35. A.A. Isse, A. Gennaro, E. Vianello, *Electrochim. Acta* 42 (1997) 2065-2069.